Optimized operation of quantum dot intermediate-band solar cells deduced from the electronic transport modelling

Nicolas Cavassilas, Daniel Suchet, Amaury Delamarre, Jean-François Guillemoles, Fabienne Michelini, Marc Bescond, Michel Lannoo

Optimized operation of quantum dot intermediate-band solar cells deduced from the electronic transport modelling

Nicolas Cavassilas,[1] Daniel Suchet,[2] Amaury Delamarre,[3] Jean-Francois Guillemoles,[4] Fabienne Michelini,[1] Marc Bescond,[5] and Michel Lannoo[1]

[1]*Aix Marseille Université, CNRS, Université de Toulon, IM2NP UMR 7334, 13397, Marseille, France*

[2]*Ecole Polytechnique, IPVF, Institut Photovoltaïque d'Ile-de-France, 30 RD 128, 91120 Palaiseau, France*

[3]*Centre de Nanosciences et de Nanotechnologies, Palaiseau, Ile-de-France, France*

[4]*IPVF, Institut Photovoltaïque d'Ile-de-France, 30 RD 128, 91120 Palaiseau, France*

[5]*LIMMS, CNRS-Institute of Industrial Science, UMI 2820, University of Tokyo, 153-8505 Tokyo, Japan*

Abstract

So far physics of quantum electronic transport has not tackled the problems raised by quantum dot intermediate-band solar cells. Our study shows that this physics imposes design rules for the inter-subband transition. We developed an analytical model that correctly treats, from a quantum point-of-view, the trade-off between the absorption, the recombination and the electronic transport occurring in this transition. Our results clearly indicate that it is essential to control the transit rate between the excited state of the quantum dot and the embedding semiconductor. For that, we propose to assume the dot in a tunnel-shell whose main characteristics can be obtained by a simple analytical formula. Moreover, we show that in a realistic case, the energy transition only needs to be larger than 0.28 eV to obtain a quasi Fermi-level splitting. This quite small value designates the quantum dot solar cell as a serious candidate to be an efficient intermediate-band solar cell. This work gives a framework to design efficient inter-subband transitions and then opens new opportunities for quantum dot intermediate-band solar cells.

I. INTRODUCTION

Inter-subband transitions are widely used in infrared sensors [1] and in the concept of intermediate-band solar cells (IBSC) [2]. From an optical point-of-view these transitions have been the subject of numerous studies which show that the monochromatic absorption is maximal between the ground state and the first excited state if those two are well localized (bound-to-bound system) [3]. Nevertheless, whether in sensors or in solar cells, the objective is to recover excited electrons in an electric current. In case of sensors this current is the response to the absorption while in a solar cell it is at the origin of the generated power. However, in the case where the electrons were excited on a very localized state, it will be difficult to withdraw them in an electrical contact. On the other hand, the reduction of the localization decreases the maximum of absorption, but also broadens it. This could be an advantage for a wide spectrum excitation. Finally, we understand that it will be necessary to find a compromise between absorption, recombination and extraction [4].

In this paper we propose an analytical model in which all these effects are considered rigorously from the point-of-view of quantum mechanics. We have developed this model based on the non-equilibrium Green functions (NEGF) formalism that allows to treat a quantum system with interactions [5–9]. The system, in this case a quantum dot with a tunnel-shell embedded in a 3D material, is simplified for computational concerns. The main simplifications are a perfectly selective contact, flat bands **and the effective mass approximation. This gives an effective model which, with a reduce number of parameters, favor the understanding of tricky but ultimately very important quantum transport phenomena. Moreover, even if such approaches are not so precise that fully numerical models, effective models are currently used to optimize devices assuming, for example, strongly confined system [10, 11], tunneling modified by strain [12] or scattering in quantum well [13].**

This analytical model is then applied to the inter-subband transition of an IBSC. The purpose of these concept is to exceed the Shockley-Queisser limit [14] by using an intermediate-band in the band-gap of the absorbing semiconductor [15, 16]. The idea is to use this intermediate-band to absorb photons having a lower energy than the energy gap. This absorption is then supposed to contribute to the current [17] without the full loss in voltage of a simple bandgap solar cell. To create an intermediate-band the use of nano-objects (usually

dots) is often adopted [2, 18, 19]. Their lowest conduction state serves as an intermediate-band while the second one is connected to the contact. But, this concept has not yet demonstrated performances beyond the Shockley-Queisser limit [19]. The main difficulty is that electronic populations in the intermediate-band and in the contact must not be allowed to equilibrate, in order to maintain a quasi-Fermi level splitting. Without this splitting, the IBSC is reduced to a simple solar cell with the bandgap defined by the energy between the valence-band and the first conduction state of the nano-objects. This is usually obtained experimentally. In this article, we deeply investigate this inter-subband transition, between the two first conduction states of the dot.

We have already reported a study dedicated to this transition [4], but conclusions were limited to a specific case (one set of parameters). With the present analytical model, it is henceforth possible to extend this study and to draw more general conclusions. We show that this transition must follow some rules, related to quantum electronic transport, in order to provide the efficiency higher than an equivalent single gap cell. To the best of our knowledge, none of these rules have ever been respected in quantum-dot IBSC proposed in the literature. Our findings, therefore, offer new perspectives by providing a framework for the design of IBSC.

II. MODEL AND SYSTEM

The system we model is schematically represented in Fig. 1. It is characterized by a discrete state $|1\rangle$ of energy E_1 filled with an energy-independent distribution f_1 which will be considered as an input parameter. This state represents the intermediate-band and f_1 the filling of this band. In an IBSC, f_1 is also relative to the transition between the valence-band and the intermediate-band. Even though this transition is another technological challenge involving the holes transport, here, we only consider it through this filling parameter. In addition to the first state $|1\rangle$, which is perfectly located in the quantum dot, we consider an excited state $|2\rangle$ at E_2 (the transition energy is given by $E_t = E_2 - E_1$) which has a coupling strength to the contact tuned *via* a tunnel barrier. The characteristics of this barrier result in a tunnel transfer rate σ_T. Tunneling can occur in both ways, either extracting generated carriers from $|2\rangle$ to the contact, or injecting carriers from the contact into $|2\rangle$ for a retrapping. As far as emission and absorption are concerned, both states $|1\rangle$ and $|2\rangle$ are linked by σ_I and

σ_S the induced and spontaneous optical transition rates respectively. Moreover, as stated in the introduction, the states $|1\rangle$, $|2\rangle$ and the contact do not share the same distribution. We then consider a second Fermi function for the contact f_c. In an illuminated IBSC the two corresponding chemical potentials μ_c and μ_1 must be split so that there is a gain compared to a single bandgap cell. **In our model this quasi-Fermi level splitting, $S = \mu_c - \mu_1$, is an input parameter.** Finally the contact is also defined by its energy band-edge E_c and we will call in the following $E_r = E_2 - E_c$ the ratchet energy [20–24].

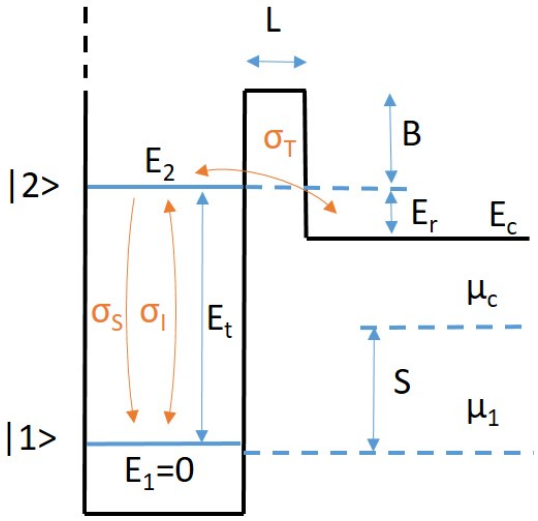

FIG. 1: Band diagram of the dot with the tunnel shell embedded in a 3D material. We assume flat bands and a perfect selected contact (infinite barrier on the left part). The input parameters are the energy E_1 of the ground-state $|1\rangle$ (the intermediate-band), the energy E_2 of the excited state $|2\rangle$, the height and the thickness of the barrier B and L respectively and E_c the energy of the band-edge of the contact. Concerning transport, the states $|1\rangle$, $|2\rangle$ and the contact are coupled by tunneling (σ_T), induced and spontaneous optical couplings (σ_I and σ_S). In all the present study, the origin of energy is $E_1 = 0$.

In order to calculate the current generated by this transition we use detailed-balance model with radiative and tunnelling rates calculated with the NEGF formalism. It is very powerful since it allows to consider a quantum system with interactions. The interaction between photons and electrons is indeed processed by a self-energy which represents the central concept to describe inelastic scattering in the Green's functions. In the literature this is usually done numerically [5, 7]. Here, by simplifying the description of the system

(through the flat bands approximation in particular), we can include it analytically. For example it allows us to calculate the tunnel transit rate from state $|2\rangle$ through the tunnel barrier:

$$\sigma_T = \frac{8E_2}{3\hbar k_r W \cosh^2(L\rho)} \tag{1}$$

with $W = \hbar\pi/(\sqrt{\frac{2E_t m^*}{3}})$ the side length of the cubic dot and L the thickness of the tunnel barrier. The wave vectors of the electron at energy E in the contact (with origin $E_1 = 0$) and the barrier are respectively given by $k_r = \sqrt{2(E_2 - E_c)m^*}/\hbar$ with m^* the effective mass, and $\rho = \sqrt{2Bm^*}/\hbar$ with B the barrier energy related to E_2. As expected this expression shows that the tunnel transit rate σ_T decreases exponentially with L. Moreover, it shows that when E_2 is close to E_c (low k_r), an interference behavior increases the tunnel rate. Note finally that this expression is original. It is indeed related, to the tunneling between a continuum and a quasi-continuum [25], and not to the tunneling between two continua or to a resonant tunneling on a bound state [26, 27].

The analytical development, to obtain this expression, is exposed in the Supplemental Material (SM), like the development of the current formula resulting in the Eq. (4) of the present work. Before to expose this full expression, we present another formula, having a close form, but obtained with a simpler development based on rate model. This toy model helps to better understand the final formula of the current.

For this toy model, we assume discrete states for $|1\rangle$, $|2\rangle$ and the contact. Moreover, σ_T and both optical rates σ_I and σ_S are independent of the energy. It is then straightforward to write the variation in time of the distribution f_2 on the state $|2\rangle$ knowing f_1 and f_c:

$$\frac{\mathrm{d}f_2}{\mathrm{d}t} = \sigma_T \{f_c(1-f_2) - f_2(1-f_c)\} + \sigma_I \{f_1(1-f_2) - f_2(1-f_1)\} - \sigma_S f_2(1-f_1). \tag{2}$$

In steady state this variation vanishes. Assuming this condition, and knowing that the current at the contact is given by $J = -e\sigma_T(f_2 - f_c)$ (e the elementary charge) we then have for the current:

$$J = e\sigma_T \frac{\sigma_I(f_c - f_1) + \sigma_S f_c(1-f_1)}{\sigma_T + \sigma_I + \sigma_S(1-f_1)}. \tag{3}$$

This expression shows that the current is a competition between induced absorption and spontaneous recombination (in the numerator). This competition is all the more favorable for absorption as f_1 is high and f_c is low. The technological challenge is to have a higher

generation than the recombination while having a higher chemical potential in the contact than in the state $|1\rangle$. Concerning the trade-off between tunneling and optic, we note that numerator is given by the product of σ_T with the summation of the optical rates, while the denominator equals the summation of all rates. Therefore, if σ_T is strongly larger than the optical rates, the current is limited by the optical processes. In the opposite situation, the current is limited by the tunneling. This then confirms that current is a balance between all such interactions.

The main limit of this toy model is that the density-of-states of $|2\rangle$ is a simple Dirac peak. This state being linked to both state $|1\rangle$ and contact, lifetime is finite. This implies, according to the relation of uncertainty, that state $|2\rangle$ is broadened [5, 28]. We will see in the following that this broadening is the key element to obtain a maximum of efficiency. By considering the calculation of the transit rates *via* the NEGF formalism, as shown in the SM, we go beyond the previous toy model (Eq. (3)) and obtain for the current across the system presented in Fig. 1, the following expression:

$$\begin{aligned} J(S) &= \int_{E_c}^{E_m} J(S,E)dE = \int_{E_c}^{E_m} (J_A(S,E) + J_R(S,E))dE \\ &= \frac{2e}{h}\int_{E_c}^{E_m} \sigma_T \frac{\sigma_I(E)(f_c(E)-f_1) + \sigma_S(E)f_c(E)(1-f_1)}{(\frac{E-E_2}{\hbar})^2 + (\sigma_T + \sigma_I(E) + \sigma_S(E)(1-f_1))^2}dE, \end{aligned} \tag{4}$$

The absorption current $J_A(S,E)$ is related to the induced optical rate $\sigma_I(E) = \frac{\mathcal{M}(E)}{\hbar}(C\Omega_S b_{T_S}(E) + n_r\pi b_{T_R}(E))$, while the retrapping current $J_R(S,E)$ is related to the spontaneous optical rate $\sigma_S(E) = \frac{\mathcal{M}(E)}{\hbar}n_r\pi$. The electron-photon coupling is given by:

$$\mathcal{M}(E) = \frac{\hbar E}{8\pi^3\epsilon_0}\left(\frac{8e}{3m^*W}\right)^2\left(\frac{n}{c}\right)^3 \tag{5}$$

with n the refractive index of the considered material, $b_T(E) = \frac{1}{\exp\frac{E}{k_BT}-1}$ the Bose distribution, $T_S = 6000$K and $T_R = 300$K respectively the sun and the room temperatures, $\Omega_S = 6.7\times10^{-5}$ the solid angle of absorption. We also have $f_c(E) = \frac{1}{1+\exp\frac{E-\mu_c}{k_BT_R}}$. Concerning the sign convention for the current, power is produced when $J < 0$. For all calculations, we choose an initial state half-filled with $f_1 = 0.5$, involving $\mu_1 = E_1$. The upper limit E_m is a numerical parameter defined in the SM. Finally, C is the sun concentration and n_r a non-radiative coefficient that accounts for non radiative recombination: for one radiative recombination we have $(n_r - 1)$ non-radiative ones. This parameter strongly depends on the materials, growing conditions and shape of the dots [29]. In consequence, while experimental study shows results close to the radiative limit [29, 30], theoretical calculations

suggest $n_r = 5 \times 10^4$ [31]. In the following, we generally assume $n_r = 10^2$ but we extended our conclusions to the radiative limit and to the case where strong non-radiative processes occur.

The denominator of Eq. (4) looks like that of a Lorentzian centered on E_2, while the numerator looks like that of Eq. (3). Indeed, in both Eqs. (3) and (4), the current is proportional to the tunnel transit rate σ_T and is a competition between absorption and retrapping. But compared to Eq. (3), the denominator of Eq. (4) shows a broadening around E_2 which is given by the sum of the different transition rates. A fast analysis of this equation shows that $J(0, E_2)$ is maximum when $\sigma_T = \sigma_I(E_2) + \sigma_S(E_2)(1 - f_1)$. If σ_T is lower, the current is limited by the tunneling, while if it is larger, the current is limited by the absorption. This condition does not involve that the current is maximal since the total current is the result of a summation over energy. However, as we will show in the following of this article, adjusting the design to fulfil this condition remains a good milestone.

We can note finally that this set of equations can easily be implemented in a few lines of code as shown in the SM. Using Eq. (4) we can calculate the current spectrum and the total current as a function of S for the junction shown in Fig. 1. If we consider this inter-subband transition as a solar cell, we can calculate the corresponding current $J_{sc} = J(S = 0)$, the quasi-Fermi level splitting canceling the current S_{oc} and the maximum power P_{max}.

III. RESULTS

Figure 2 shows current spectra at S_{oc} for a realistic set of parameters and different tunnel barrier thicknesses. The negative (positive) component corresponds to absorption (retrapping). The narrower around E_2 these two components are, the thicker is the barrier. This reflects the effect of the lifetime on the broadening of $|2\rangle$ controlled by the tunnel rate. For recombination, in addition to this peak, there are also electrons injected from the contact band-edge at E_c. This contribution is all the more important as the broadening of $|2\rangle$ is important. Indeed, a high density-of-states in the well at the energy E_c promotes the injection from the contact. In the bound-to-continuum case ($L = 0$ nm) shown in Fig. 2a, the broadening is maximum and this band-edge injection is dominant. As a result, S_{oc} is low since it is controlled by E_c and not by E_2. This band-edge also impacts the current absorption since, as shown Fig. 2a, the spectrum is cut-off at E_c. Therefore, in case of large

broadening of $|2\rangle$, the effective energy transition is more defined by E_c than by E_2 in sense that a low (high) E_c means a high (low) J_{sc} and a low (high) S_{oc}.

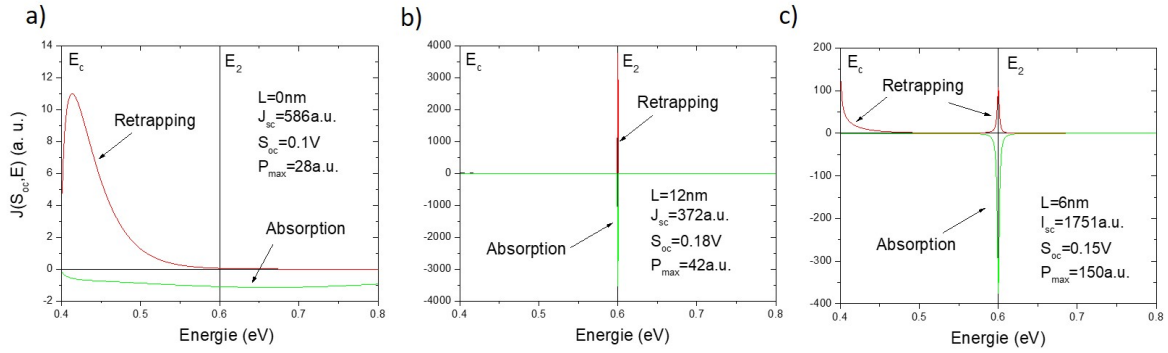

FIG. 2: Current spectrum, calculated at S_{oc}, for $B = 0.2$ eV, $m^* = 0.07m_0$ (m_0 the free electron mass), $n = 3.5$, $n_r = 10^2$, $E_t = 0.6$ eV, $E_r = 0.2$ eV, $E_m = 1.4$ eV, a) $L = 0$ nm, b) $L = 10$ nm and c) $L = 5$ nm. The absorption current $J_A(S_{oc}, E)$ is represented by the green line and the retrapping current $J_R(S_{oc}, E)$ by the red line. For each value of L we also show J_{sc}, S_{oc} and P_{max}.

Figure 2b shows the current spectrum in the bound-to-bound case with a thick barrier, $L = 10$ nm. The broadening being small we just have a very weak injection from E_c and consequently a higher S_{oc} than in the bound-to-continuum case. We recover here the *broadening effect* introduced in a previous work [4] at the origin of S_{oc} modification. Moreover, the excitation component being very narrow around E_2, the absorption spectrum is no-more cut-off at E_c. In this case, the effective energy of the inter-subband transition is defined by E_2. However, despite a higher S_{oc}, the power is just a little larger than in the bound-to-continuum case. The current is indeed limited since the excited electrons hardly tunnel through the contact. The best trade-off between absorption, extraction and recombination, is obtained for the intermediate case shown Fig. 2c where $L = 5$ nm. The consequence of the corresponding moderate broadening is a much larger current and an intermediate S_{oc}. Compared to the usually assumed bound-to-bound case, the current and the power are increased by ratio of 3 and 5, respectively.

These results show that it is essential to control the broadening of the state $|2\rangle$ via σ_T to have a good balance between all transport processes. For that, as we had already suggested in Ref. [4], a well-designed tunnel barrier is a relevant solution. While the bound-to-continuum case is generally considered in IBSC [32–35], some studies assume the quantum

dot embedded in a high bandgap material [36–40]. This last solution is proposed to reduce the strain and the corresponding structural defects, but it could also make it possible to control the tunnel transit and hence the broadening of the excited state. It is also possible to design a dot directly in the host-material, without shell, if both the band-offset and the dot size are sufficient to have a localized excited state. In this case, the tunnel barrier between the dot and the contact has to be controlled by an electric field generated by doping and/or build-in charge [41].

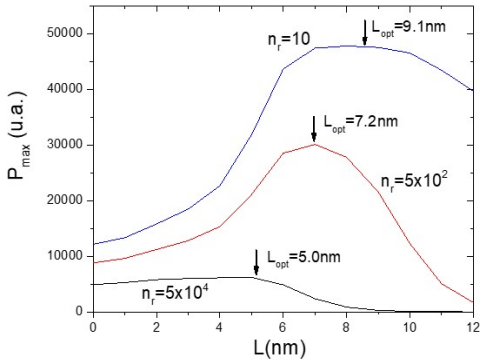

FIG. 3: Maximum power P_{max} *versus* the tunnel barrier thickness L extracted form the $J-V$ characteristic calculated with Eq. (4) for $B = 0.2$ eV, $m^* = 0.07m_0$ (m_0 the free electron mass), $n = 3.5$, $E_t = 0.6$ eV, $E_r = 20$ meV, $C = 500$ and various n_r. We also report the estimation of the optimal thickness L_{opt} obtain with Eq. (6). In order to estimate the precision of this equation, these values can be compared to the top position of the corresponding curves.

The optimal barrier thickness depends on all parameters and the precedent value of 5 nm cannot be generalized. In order to offer an extended study, it would be interesting to have an expression estimating such an optimal barrier thickness. For that, we remember that the current $J(0, E_2)$ is maximum when $\sigma_T(E_2) = \sigma_I(E_2) + \sigma_S(E_2)(1 - f_1)$, and checking that $\sigma_I \ll \sigma_S$, we propose an expression allowing to approximately estimate the best trade-off: $\sigma_T(E_2) = \alpha(n_r)\sigma_S(E_c)$ with $\alpha(n_r) = 60 \times \exp(\log 10(n_r) - 1)$. Considering this condition in Eq. (4), we extract an expression which estimates the value of the optimal thickness of the tunnel barrier, L_{opt}, according to all the other parameters:

$$L_{opt} = \frac{1}{\rho}\ln\left(\frac{\sqrt{\frac{8E_t}{3k_rW}} + \sqrt{\frac{8E_t}{3k_rW} - M(E_c)\pi n_r\alpha(n_r)(1-f_1)}}{\sqrt{M(E_c)\pi n_r\alpha(n_r)(1-f_1)}}\right). \quad (6)$$

This expression shows that, for example, in case of large non-radiative coefficient n_r and/or low f_1, the retrapping is naturally large and L should be chosen small in order to preserve a large σ_T. At the opposite, close to the radiative limit, L should be large. We note also that all parameters modifying σ_T also play a role, which includes k_r related to the ratchet energy, E_t and W both related to the dot design. Figure 3 illustrates the impact of the recombination by representing the maximum power *versus* L (calculated with the Eq. (4)) for various n_r. These curves, in addition to illustrating the advantage of considering a tunnel barrier, confirm the good estimation of L_{opt} given by Eq. (6).

TABLE I: The minima of energy for the intermediate-band / conduction band transition calculated for several concentration C and non-radiative coefficient n_r. E_{quant}, calculated with our model, corresponds to the limit under which the inter-subband transition cannot produce power. $E_{classic}$ calculated with a detailed-balance model assuming sharp absorption, corresponds to the limit under which the IBSC is less efficient that the optimal single bandgap cell.

C	n_r	1	10^2	5×10^4
1	E_{quant}	0.15	0.27	0.43
	$E_{classic}$	0.14	0.30	0.49
500	E_{quant}		0.11	0.27
	$E_{classic}$		0.08	0.30
10^4	E_{quant}		0.03	0.19
	$E_{classic}$		0.02	0.20

Finally, we can estimate thanks to our model, the minimum of the transition energy allowing the generation of a power with the considered inter-subband transition. Indeed, reducing E_t and consequently E_c involves an increase of the injection from the contact. If, at $V = 0$V, the retrapping current is of the same order of magnitude than the absorption current, application of any quasi-Fermi level splitting is impossible. For example, for $n_r = 10^2$ and $C = 1$ we find that E_t has to be larger than 0.28 eV. We calculate this limit, called E_{quant}, for several concentrations and non-radiative factors as shown in Table I.

Regardless of the present study, the optical transitions in IBSCs must be large enough for such cells to offer higher efficiency than the optimal single bandgap cell. **This limit can be**

estimated with a classical detailed-balance model (described in SM) considering the three optical transitions of the IBSC [24]. In Table I, we compare this classical limit $E_{classic}$ with the quantum limit E_{quant}. These two limits are, in any case, very close. This means that the inter-subband character of the transition, if it is well designed, does not increase the limitation to obtain an efficient IBSC. This validates the use of quantum dots as a judicious choice for the IBSC.

IV. CONCLUSION

In conclusion, we have presented a theoretical study on the inter-subband transition in quantum dot IBSCs. For this, we have developed a rigorous model, but nevertheless easy to implement. Using this model, we can give recommendations for designing an efficient inter-subband transition. Considering a realistic recombination rate, the transition energy E_t between the intermediate-band and the excited state must be higher than 0.28 eV without concentration and 0.13 eV under 500 suns. Under this limit, the intermediate-band is at the thermodynamic equilibrium with the contact. Above this limit, the tunnel rate has to be controlled by a tunnel barrier. In the radiative limit, this barrier should be thick, while it should be all the thinner when the non-radiative processes increase. In case where the optimal design suggests a thick barrier, an energy ratchet may be considered without any damage because tunneling from E_c to the dot is reduced. Such a ratchet could represent an advantage, since as we saw in another study [22, 23], degrees-of-freedom on E_r make it possible to match the different transitions of the IBSC. On the other hand, in case of thin barrier, both S_{oc} and J_{sc} are controlled by such a ratchet energy. This parameter has then to be carefully chosen using the Eq. (4) of this letter.

This study confirms that obtaining an efficient IBSC involves significant technological challenges, particularly for the band offsets in order to achieve a sufficiently large E_t. On the other hand, we show that the inter-subband character of the transition does not worsen these conditions and we confirm that the quasi-Fermi level splitting can be achieved, even if the non-radiative processes are huge.

Finally, it is important to note that the analytical model presented in this work is not only dedicated to the IBSC. It may also be useful for other devices assuming an inter-subband transition such as photodetector or laser.

Acknowledgement

The authors thank ICEMAN (ANR-19-CE05-000) for financial support.

---

[1] P.-B. Vigneron, S. Pirotta, I. Carusotto, N.-L. Tran, G. Biasiol, J.-M. Manceau, A. Bousseksou, and R. Colombelli, Applied Physics Letters **114**, 131104 (2019), ISSN 0003-6951, 1077-3118, URL http://aip.scitation.org/doi/10.1063/1.5084112.

[2] S. Tomic, T. Sogabe, and Y. Okada, Progress in Photovoltaics: Research and Applications **23**, 546 (2015), ISSN 10627995, URL http://doi.wiley.com/10.1002/pip.2455.

[3] B. F. Levine, A. Zussman, S. D. Gunapala, M. T. Asom, J. M. Kuo, and W. S. Hobson, Journal of Applied Physics **72**, 4429 (1992), ISSN 0021-8979, 1089-7550, URL http://aip.scitation.org/doi/10.1063/1.352210.

[4] N. Cavassilas, D. Suchet, A. Delamarre, F. Michelini, M. Bescond, Y. Okada, M. Sugiyama, and J.-F. Guillemoles, EPJ Photovoltaics **9**, 11 (2018), ISSN 2105-0716, URL https://www.epj-pv.org/10.1051/epjpv/2018009.

[5] N. Cavassilas, F. Michelini, and M. Bescond, Journal of Renewable and Sustainable Energy **6**, 011203 (2013), URL http://aip.scitation.org/doi/abs/10.1063/1.4828366.

[6] N. Cavassilas, F. Michelini, and M. Bescond, Journal of Computational Electronics **15**, 1233 (2016), ISSN 1569-8025, 1572-8137, URL https://link.springer.com/article/10.1007/s10825-016-0883-5.

[7] U. Aeberhard and U. Rau, Physical Review Letters **118**, 247702 (2017), URL https://link.aps.org/doi/10.1103/PhysRevLett.118.247702.

[8] A. Berbezier and U. Aeberhard, Physical Review Applied **4** (2015), ISSN 2331-7019, URL https://link.aps.org/doi/10.1103/PhysRevApplied.4.044008.

[9] M. Luisier, A. Szabo, C. Stieger, C. Klinkert, S. Bruck, A. Jain, and L. Novotny (IEEE, 2016), pp. 5.4.1–5.4.4, ISBN 978-1-5090-3902-9, URL http://ieeexplore.ieee.org/document/7838353/.

[10] K. Nehari, M. Lannoo, F. Michelini, N. Cavassilas, M. Bescond, and J. L. Autran, Applied Physics Letters **93**, 092103 (2008), ISSN 0003-6951, 1077-3118, URL http://aip.scitation.org/doi/10.1063/1.2978196.

[11] C. Medina-Bailon, T. Sadi, M. Nedjalkov, H. Carrillo-Nunez, J. Lee, O. Badami, V. Georgiev, S. Selberherr, and A. Asenov, IEEE Electron Device Letters **40**, 1571 (2019), ISSN 0741-3106, 1558-0563, URL https://ieeexplore.ieee.org/document/8792952/.

[12] L. Liu, R. Liang, J. Wang, and J. Xu, Journal of Applied Physics **117**, 184501 (2015), ISSN 0021-8979, 1089-7550, URL http://aip.scitation.org/doi/10.1063/1.4921107.

[13] A. Yangui, M. Bescond, T. Yan, N. Nagai, and K. Hirakawa, Nature Communications **10** (2019), ISSN 2041-1723, URL http://www.nature.com/articles/s41467-019-12488-9.

[14] W. Shockley and H. J. Queisser, Journal of Applied Physics **32**, 510 (1961), ISSN 0021-8979, URL http://aip.scitation.org/doi/abs/10.1063/1.1736034.

[15] A. Luque, A. Mart, and C. Stanley, Nature Photonics **6**, 146 (2012), ISSN 1749-4885, URL http://www.nature.com/nphoton/journal/v6/n3/full/nphoton.2012.1.html.

[16] A. Luque and A. Mart, Physical Review Letters **78**, 5014 (1997), URL https://link.aps.org/doi/10.1103/PhysRevLett.78.5014.

[17] N. Lopez, K. M. Yu, T. Tanaka, and W. Walukiewicz, Advanced Energy Materials **6**, 1501820 (2016), ISSN 16146832, URL http://doi.wiley.com/10.1002/aenm.201501820.

[18] T. Sogabe, Y. Shoji, M. Ohba, K. Yoshida, R. Tamaki, H.-F. Hong, C.-H. Wu, C.-T. Kuo, S. Tomi, and Y. Okada, Scientific Reports **4**, srep04792 (2014), ISSN 2045-2322, URL https://www.nature.com/articles/srep04792.

[19] Y. Okada, N. J. Ekins-Daukes, T. Kita, R. Tamaki, M. Yoshida, A. Pusch, O. Hess, C. C. Phillips, D. J. Farrell, K. Yoshida, et al., Applied Physics Reviews **2**, 021302 (2015), URL http://aip.scitation.org/doi/abs/10.1063/1.4916561.

[20] A. Pusch and N. J. Ekins-Daukes, Physical Review Applied **12** (2019), ISSN 2331-7019, URL https://link.aps.org/doi/10.1103/PhysRevApplied.12.044055.

[21] A. Pusch, M. Yoshida, N. P. Hylton, A. Mellor, C. C. Phillips, O. Hess, and N. J. Ekins-Daukes, Progress in Photovoltaics: Research and Applications **24**, 656 (2016), ISSN 1099-159X, URL http://onlinelibrary.wiley.com/doi/10.1002/pip.2751/abstract.

[22] A. Delamarre, D. Suchet, M. Sugiyama, N. Cavassilas, Y. Okada, and J.-F. Guillemoles (SPIE, 2018), p. 27, ISBN 978-1-5106-1539-7 978-1-5106-1540-3, URL https://www.spiedigitallibrary.org/conference-proceedings-of-spie/10527/2287716/Non-ideal-nanostructured-intermediate-band-solar-cells-with-an-electronic/10.1117/12.2287716.full.

[23] D. Suchet, A. Delamarre, N. Cavassilas, Z. Jehl, Y. Okada, M. Sugiyama, and J.-F. Guillemoles, Progress in Photovoltaics: Research and Applications **26**, 800 (2018), ISSN 10627995, URL http://doi.wiley.com/10.1002/pip.3020.

[24] A. Delamarre, D. Suchet, N. Cavassilas, Y. Okada, M. Sugiyama, and J.-F. Guillemoles, IEEE Journal of Photovoltaics **8**, 1553 (2018), ISSN 2156-3381, 2156-3403, URL https://ieeexplore.ieee.org/document/8454772/.

[25] R. Clerc, A. Spinelli, G. Ghibaudo, and G. Pananakakis, Journal of Applied Physics **91**, 1400 (2002), ISSN 0021-8979, 1089-7550, URL http://aip.scitation.org/doi/10.1063/1.1427398.

[26] A. Pan and C. O. Chui, Journal of Applied Physics **116**, 054509 (2014), ISSN 0021-8979, 1089-7550, URL http://aip.scitation.org/doi/10.1063/1.4891528.

[27] A. Pan and C. O. Chui, Journal of Applied Physics **116**, 054508 (2014), ISSN 0021-8979, 1089-7550, URL http://aip.scitation.org/doi/10.1063/1.4891527.

[28] G. Bastard, *Wave mechanics applied to semiconductor heterostructures*, Monographies de physique (Les ditions de Physique, 1988), ISBN 978-0-470-21708-5, URL https://books.google.fr/books?id=5rrvAAAAMAAJ.

[29] B. D. Gerardot, D. Brunner, P. A. Dalgarno, P. hberg, S. Seidl, M. Kroner, K. Karrai, N. G. Stoltz, P. M. Petroff, and R. J. Warburton, Nature **451**, 441 (2008), ISSN 0028-0836, 1476-4687, URL http://www.nature.com/articles/nature06472.

[30] G. A. Narvaez, G. Bester, and A. Zunger, Physical Review B **74** (2006), ISSN 1098-0121, 1550-235X, URL https://link.aps.org/doi/10.1103/PhysRevB.74.075403.

[31] S. Tomic, Physical Review B **82** (2010), ISSN 1098-0121, 1550-235X, URL https://link.aps.org/doi/10.1103/PhysRevB.82.195321.

[32] D. Guimard, R. Morihara, D. Bordel, K. Tanabe, Y. Wakayama, M. Nishioka, and Y. Arakawa, Applied Physics Letters **96**, 203507 (2010), ISSN 0003-6951, 1077-3118, URL http://aip.scitation.org/doi/10.1063/1.3427392.

[33] F. K. Tutu, J. Wu, P. Lam, M. Tang, N. Miyashita, Y. Okada, J. Wilson, R. Allison, and H. Liu, Applied Physics Letters **103**, 043901 (2013), ISSN 0003-6951, 1077-3118, URL http://aip.scitation.org/doi/10.1063/1.4816503.

[34] P. Lam, S. Hatch, J. Wu, M. Tang, V. G. Dorogan, Y. I. Mazur, G. J. Salamo, I. Ramiro, A. Seeds, and H. Liu, Nano Energy **6**, 159 (2014), ISSN 22112855, URL https://linkinghub.

elsevier.com/retrieve/pii/S2211285514000548.

[35] N. S. Beattie, P. See, G. Zoppi, P. M. Ushasree, M. Duchamp, I. Farrer, D. A. Ritchie, and S. Tomi, ACS Photonics **4**, 2745 (2017), ISSN 2330-4022, 2330-4022, URL https://pubs.acs.org/doi/10.1021/acsphotonics.7b00673.

[36] G. Wei and S. R. Forrest, Nano Letters **7**, 218 (2007), ISSN 1530-6984, 1530-6992, URL https://pubs.acs.org/doi/10.1021/nl062564s.

[37] S. M. Hubbard, C. D. Cress, C. G. Bailey, R. P. Raffaelle, S. G. Bailey, and D. M. Wilt, Applied Physics Letters **92**, 123512 (2008), ISSN 0003-6951, 1077-3118, URL http://aip.scitation.org/doi/10.1063/1.2903699.

[38] C. G. Bailey, D. V. Forbes, R. P. Raffaelle, and S. M. Hubbard, Applied Physics Letters **98**, 163105 (2011), ISSN 0003-6951, 1077-3118, URL http://aip.scitation.org/doi/10.1063/1.3580765.

[39] C. G. Bailey, D. V. Forbes, S. J. Polly, Z. S. Bittner, Y. Dai, C. Mackos, R. P. Raffaelle, and S. M. Hubbard, IEEE Journal of Photovoltaics **2**, 269 (2012), ISSN 2156-3381, 2156-3403, URL http://ieeexplore.ieee.org/document/6179500/.

[40] A. Varghese, M. Yakimov, V. Tokranov, V. Mitin, K. Sablon, A. Sergeev, and S. Oktyabrsky, Nanoscale **8**, 7248 (2016), ISSN 2040-3364, 2040-3372, URL http://xlink.rsc.org/?DOI=C5NR07774E.

[41] K. A. Sablon, J. W. Little, V. Mitin, A. Sergeev, N. Vagidov, and K. Reinhardt, Nano Letters **11**, 2311 (2011), ISSN 1530-6984, 1530-6992, URL https://pubs.acs.org/doi/10.1021/nl200543v.